Journal of Neuroscience Methods 206 (2012) 78–82

Contents lists available at SciVerse ScienceDirect

Journal of Neuroscience Methods

journal homepage: www.elsevier.com/locate/jneumeth

Basic Neuroscience
Short communication

# Calcium imaging of multiple neurons in freely behaving *C. elegans*

Maohua Zheng[a], Pengxiu Cao[a], Jiong Yang[b], X.Z. Shawn Xu[d,e,*], Zhaoyang Feng[a,b,c,**]

[a] *Department of Pharmacology, Case Western Reserve University, Cleveland, OH 44106, USA*
[b] *Department of Electronic Engineering & Computer Science, Case Western Reserve University, Cleveland, OH 44106, USA*
[c] *Department of Physiology, College of Medicine, Xi'an Jiaotong University, Xi'an, Shaanxi 710061, China*
[d] *Life Sciences Institute, University of Michigan, Ann Arbor, MI 48109, USA*
[e] *Department of Molecular & Integrative Physiology, University of Michigan, Ann Arbor, MI 48109, USA*

ARTICLE INFO

*Article history:*
Received 30 September 2011
Received in revised form
29 December 2011
Accepted 4 January 2012

*Keywords:*
*C. elegans*
Neuron
Behavior

ABSTRACT

*Caenorhabditis elegans* is a popular model organism to study how neural circuits and genes regulate behavior. To reliably correlate circuit function with behavior, it is important to record neuronal activity in freely behaving worms. As neural circuits are composed of multiple neurons that cooperate to process information, it is highly desirable to simultaneously record the activity of multiple neurons in the circuitry. However, such a system has not been available in *C. elegans*. Here, we report the CARIBN II (*Ca*lcium *R*atiometric *I*maging of *B*ehaving *N*ematodes version *II*) system. This system provides smoother data collection and more importantly permits simultaneous imaging of calcium transients from multiple neurons in freely behaving worms. Using this system, we imaged the activity of AVA and RIM, two key neurons in the locomotion circuitry that regulate backward movement (reversal) in locomotion behavior. We found that AVA activity increases while RIM activity decreases during the same reversal events in spontaneous locomotion, consistent with the recent report that the AVA and RIM are involved in promoting the initiation of reversals. The CARIBN II system provides a valuable tool for dissecting the neural basis of behavior in *C. elegans*.



## 1. Introduction

*Caenorhabditis elegans* expresses complex behaviors that are controlled by a relatively simple nervous system consisting of merely 302 neurons (White et al., 1986). *C. elegans* also represents the only organism with the wiring diagram of its entire nervous system completely reconstructed at the electron-microscopy (EM) level (White et al., 1986). These features in conjunction with its amenability to genetic manipulation make *C. elegans* a popular model organism for investigating how neural circuits and genes generate behavior (Barr, 2003; Mori et al., 2004; Whittaker and Sternberg, 2004). Indeed, recent studies show that some of the basic principles governing sensory processing and sensory-motor integration in *C. elegans* display surprising similarities to those found in mammals (Chalasani et al., 2007; Piggott et al., 2011).

Calcium imaging has approved to be a powerful, convenient means to record neuronal activity in many organisms. In *C. elegans*, this is further facilitated by the use of genetically encoded calcium sensors, such as G-CaMP and cameleon, as well as the transparency of the worm body, making it possible to perform calcium imaging in a non-invasive manner (Kerr et al., 2000).

To map the neural circuits underlying behavior, it is important to reliably correlate circuit function with behavioral states, which makes it necessary to record neuronal activity in freely behaving animals. To this end, we and others have recently developed calcium imaging systems that enable imaging of calcium transients of individual neurons in freely moving worms (Ben Arous et al., 2010; Piggott et al., 2011). We named our system CARIBN (*Ca*lcium *R*atiometric *I*maging of *B*ehaving *N*ematodes) system (Piggott et al., 2011). Using this system, we found that the AVA command interneuron and the RIM inter/motor neuron form parallel circuits to promote the initiation of backward movement (reversal) during locomotion (Piggott et al., 2011).

However, the functionality of the current imaging systems is still limited. For example, because of the uneven surface of the culturing plates on which worms are assayed for behavior, animals often go out of focus during locomotion and one would have to manually re-adjust the focus drive of the microscope rather frequently (Ben Arous et al., 2010; Piggott et al., 2011), a task that is tedious and also highly prone to human errors. An autofocus function would be highly beneficial. In addition, the current systems can only image the neurons on the same focal plane (Ben Arous et al., 2010; Piggott et al., 2011). In most cases, one can only image one single neuron at

* Corresponding author at: Life Sciences Institute, University of Michigan, Ann Arbor, MI 48109, USA. Tel.: +1 734 615 9311.
** Corresponding author at: Department of Pharmacology, Case Western Reserve University, Cleveland, OH 44106, USA.
*E-mail addresses:* shawnxu@umich.edu (X.Z.S. Xu), john.feng@case.edu (Z. Feng).

0165-0270/$ – see front matter © 2012 Elsevier B.V. All rights reserved.
doi:10.1016/j.jneumeth.2012.01.002

the time. As neural circuits are composed of multiple neurons that function cooperatively to process information, it is highly desirable to simultaneously record the activity of multiple neurons in the circuitry. Here, we report the CARIBN II (CARIBN version II) system that incorporates autofocus and *z*-sectioning functions, thereby allowing smoother data collection and simultaneous imaging of multiple neurons in freely behaving worms. Using CARIBN II, we found that the activity of AVA and RIM but not AVD is associated with the same reversal events, consistent with a recent model (Piggott et al., 2011). CARIBN II is a useful tool that facilitates the dissection of the neural basis of behavior in *C. elegans*.

## 2. Materials and methods

### 2.1. The CARIBN II system

The hardware of the system is described in Section 3 and Fig. 1a. It is identical to that described previously except the stage (Piggott et al., 2011). We developed software (see Section 3) to control the hardware system to follow fluorescent objects in dark field based on their size and brightness, which was developed on top of the original CARIBN system (Piggott et al., 2011). The original CARIBN system does not control the *z*-axis to allow autofocus or *z*-sectioning. To accomplish these functions, we introduced two new modules in CARIBN II (see Section 3). Software was written with ANSI standard C, NI Vision library, NI LabWindow CVI (National Instruments), complied and benchmarked on a Dell OptiPlex 380 desktop computer (Dell), and is available upon request. The imaging conditions were identical to those described previously (Piggott et al., 2011). To isolate neurons for ratio computation, we generated a mask image for each frame by applying several digital filters, including a spatial filter (sharpening the image), an intensity filter and size filter (isolating the neuron from others and the nerve ring). Specifically, image sharpening was achieved by applying the NI image median filter. This non-linear filter assigns each pixel the median value of its neighborhood specified by a given filter size ($3 \times 3$ pixel) to improve the edges between fluorescent objects and background, thereby sharpening the images. It should be noted that though this filter helps isolate neurons for ratio computation, it does not alter the value of G-CaMP/DsRed fluorescence ratio, because ratio computation was based on the raw images. The threshold for the intensity filter was set as the mean value of background intensity plus $3\times$ SD (standard deviation). A pixel with an intensity value greater than this threshold was considered part of the object (neuron). The size filter was typically set as 15 pixels or a value chosen by the user. To quantify the ratio change in a reversal event, we first determined the precise starting and ending frames of the event. We used the mean ratio value derived from the frames spanning ~2 s before the starting frame as the basal line value, and the value from the first main peak or trough of the reversal event was used to calculate the ratio change.

### 2.2. Nematode strains and calcium imaging experiments

Transgenic lines co-expressing G-CaMP3.0 and DsRed2 (Clonetech) and the calcium imaging protocols were described previously (Piggott et al., 2011). The transgene was driven by the *nmr-1* promoter (Zheng et al., 1999). Briefly, day 1 adults were randomly selected from the stocking plates and transferred onto an NGM plate freshly seeded with a thin layer of freshly grown OP50 bacteria (Cao et al., 2010). During imaging, worms were allowed to freely move on the surface of the NGM plate in an open environment without any physical restraint. All imaging experiments were carried out on *lite-1(xu7)* worms that lack intrinsic phototactic responses to short wavelength light (Liu et al., 2010; Ward et al., 2008).

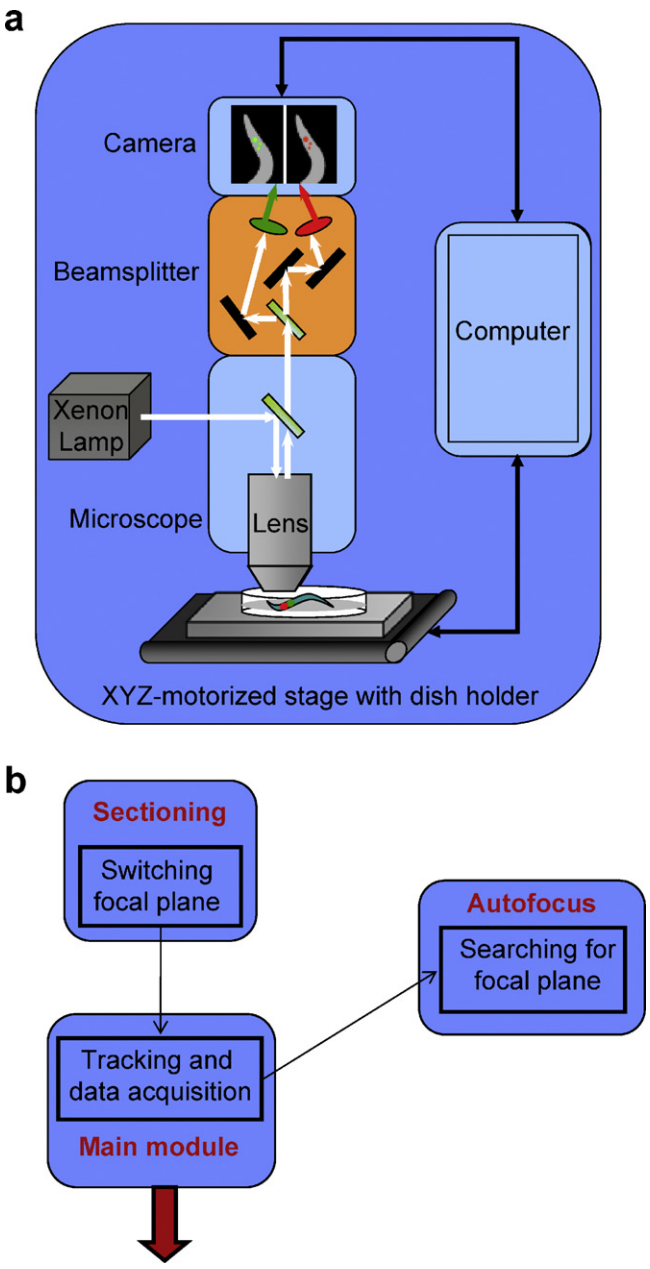


**Fig. 1.** Hardware and software of CARIBN II. (a) Schematic diagram of the hardware. (b) Schematic diagram of the software.

## 3. Results and discussion

### 3.1. The CARIBN II system

Fig. 1a describes the hardware of CARIBN II. It consists of an upright microscope (SV11, Carl Zeiss), a dual-view beamsplitter (Optical Insights), an Electron Multiplying Charge Coupled Device (EMCCD) camera (Andor Technology), a Xenon light source (Sutter Instruments) and a motorized stage with a Petri dish holder (Fig. 1a). The stage is equipped with a motorized *xyz*-axis, allowing program-controlled *z*-axis sectioning to image neurons located at different focal planes, as well as autofocus. A dual band excitation filter (Chroma Technology, U.S.A.) simultaneously excites the genetically encoded calcium sensor G-CaMP and DsRed2 at 488 nm and 560 nm, respectively. The introduction of DsRed2, a calcium-insensitive fluorescent protein marker, enables ratiometric imaging (Feng et al., 2006). A $20\times$ objective lens was

used in conjunction with a 1.6× zoom lens to image nematodes.

The software package of CARIBN II includes CARIBN-Tracker and CARIBN-Miner, two standalone software developed on top of similar components of CARIBN. CARIBN-Tracker controls hardware to track fluorescent objects. It also collects and saves visual/motion data and other necessary information. CARIBN-Miner retrieves and processes data to compute the ratio of G-CaMP/DsRed fluorescence. CARIBN-Miner remains largely the same as that of CARIBN. To enable autofocus and imaging of multiple neurons at different focal planes, we added two new modules (i.e. sectioning and autofocus) to CARIBN-Tracker on top of the main module (Fig. 1b). Thus, CARIBN-Tracker consists of three modules (Fig. 1b).

During imaging, three modules run in a multiple-thread mode, i.e., multiple tasks are executed in parallel (Fig. 1b). The main module conducts data acquisition, tracks fluorescent objects, acquires visual data, *x*–*y* motion data and *z*-axis focal plane data, and then saves these data to the hard drive of the computer. The second module performs autofocus, which is achieved by positioning the dish holder along *z*-axis to search for the focal plane at which the image of the object of interest displays the highest contrast. The third module sections nematodes transversely to switch between two defined focal planes by positioning the dish holder up or down along motorized *z*-axis.

### 3.2. Imaging AVA and RIM in freely moving worms using CARIBN II

To test the CARIBN II system, we focused on the locomotion behavior, one of the most prominent behaviors in *C. elegans*. Animals were imaged on the surface of an NGM plate in an open environment without any physical restraint, which is the standard laboratory condition under which nearly all behavioral assays in *C. elegans* are conducted. We first examined its autofocus function and found that it can actively re-adjust the *z*-axis of the stage to keep the fluorescent objects in focus. Specifically, we manually turned the focus drive to slightly defocus the image (Fig. 2a, left panel). CARIBN II quickly detected this defect and re-focused the image (Fig. 2a, right panel). The image also appeared brighter and sharper, indicative of higher signal-to-noise (Fig. 2a, right panel). Among a total of 60 such trials performed on 5 animals, CARIBN II caught all these events and re-focused the image in all cases within $185 \pm 10$ ms. As the data acquisition rate was 22 Hz without binning, this would lead to a loss of 4 frames at most. This is, however, an overestimation, as we found that during the actual experiment, CARIBN II only had to perform such a task once every ~5 s, which would only result in a loss of ~1 frame rate. However, without this function, it is common that seconds of data could get lost in a typical 2 min experiment. Thus, this new function not only improved image quality and minimized the loss of frames which was frequently experienced by the prototypic CARIBN system, but also made it unnecessary to manually adjust the focus, which is rather tedious and error-prone.

We then tested the *z*-sectioning function of CARIBN II. During spontaneous locomotion, worms spend most of their moving forward or dwelling but occasionally engage in backward movement (reversal) to change the direction of locomotion (Zhang et al., 2011). A group of command interneurons (AVA, AVD and AVE) are known to be important for the initiation of reversals, among which AVA has been shown to play a major role (Chalfie et al., 1985; Gray et al., 2005; Zheng et al., 1999). In addition, another inter/motor neuron RIM acts in parallel to AVA to trigger reversals (Piggott et al., 2011). AVA and RIM trigger reversals through distinct mechanisms. Specifically, stimulation of AVA triggers reversals, presumably through its activation of downstream ventral cord motor neurons (Gray et al., 2005; Piggott et al., 2011; Zheng et al., 1999). On the other hand, RIM inhibits reversals through some unknown motor neurons and/or muscles, and ablation of RIM increases the frequency of reversals (Alkema et al., 2005; Gray et al., 2005; Piggott et al., 2011; Zheng et al., 1999). Inhibition of RIM activity disinhibits this inhibition, leading to reversal initiation (Piggott et al., 2011). Previous calcium imaging results show that AVA increases its activity (Ben Arous et al., 2010; Faumont et al., 2011; Kawano et al., 2011; Piggott et al., 2011), while RIM decreases its activity during spontaneous reversals (Piggott et al., 2011), consistent with the view that both AVA and RIM contribute to reversal initiation in spontaneous locomotion (Piggott et al., 2011). However, this conclusion was inferred from the data that were acquired by imaging AVA and RIM separately in different reversals. Thus, the possibility that AVA and RIM may not be functional in the same reversals cannot be excluded. The CARIBN II system offers an opportunity to test this model by imaging these two neurons in the same reversals.

We used a G-CaMP transgene that consistently labels AVA, RIM and AVD in the head ganglion (Piggott et al., 2011). Under our conditions, AVA and AVD can usually be detected on the same focal plane (Fig. 2b, left panel). RIM, however, is on a different focal plane (Fig. 2b, right panel). Thus, RIM appeared very dim and often invisible on the focal plane of AVA and AVD (Fig. 2b, left panel). On the other hand, as AVA and AVD were brighter than RIM, they could still be detected on the RIM focal plan but were not in perfect focus (Fig. 2b, right panel). We first attempted to image AVA, RIM and AVD in a fixed focal plane that captured all three neurons without enabling the *z*-sectioning function. We also disabled the autofocus function, as the system would otherwise automatically focus on the brightest neuron AVA. Thus, under this condition (no autofocus or *z*-sectioning), all three neurons were not in perfect focus. Nevertheless, we found that an increase in AVA calcium level was associated with reversals (Fig. 2c). By contrast, consistent with a recent report (Kawano et al., 2011), we also failed to detect a calcium signal in AVD that was correlated with reversals (data not shown). This supports the view that AVD plays a minor role in spontaneous reversals (Chalfie et al., 1985; Gray et al., 2005; Piggott et al., 2011; Zheng et al., 1999). In the same reversal event, we also detected a decrease in RIM activity in freely behaving worms (Fig. 2c), indicating that AVA and RIM show activity in the same reversals.

Interestingly, when worms were imaged under a cover glass, we detected an increase rather than a decrease in RIM activity during reversals, consistent with a recent report (Kawano et al., 2011; data not shown). As reported previously (Piggott et al., 2011), the excitatory input to RIM is likely to be derived from AVA/AVD/AVE via gap junctions that are differentially regulated under different behavioral contexts (Piggott et al., 2011). Perhaps under a cover glass, worms have to overcome extra resistance imposed by the overlying cover glass to move around, which may lead to activation of the gap junctions between RIM and AVA. Apparently, different imaging conditions may yield different results.

Although we were able to detect signals in RIM during reversals, as RIM was dim under this condition (no autofocus or *z*-sectioning), the signals in RIM were rather noisy and the ratio change was not robust (Fig. 2c). Although this data seems to be consistent with the notion that AVA and RIM act in the same reversals, the low data quality prevented us from drawing a strong conclusion. We therefore tested our *z*-sectioning function. Under this imaging mode, the autofocus function was also enabled. We found that RIM appeared brighter and sharper in its own focal plane (Fig. 2b, right panel). We detected robust AVA and RIM signals, with both neurons showing a ratio change twice of that detected without the use of the *z*-sectioning and autofocus functions (Fig. 2d and e). For some unknown reason, the kinetics for RIM signals also seem to be improved (Fig. 2d). One possibility is that the autofocus function might have contributed. Indeed, under the autofocus mode (but the *z*-sectioning function was off), the kinetics of RIM calcium transients also seemed to be improved (Fig. S1). It is a bit

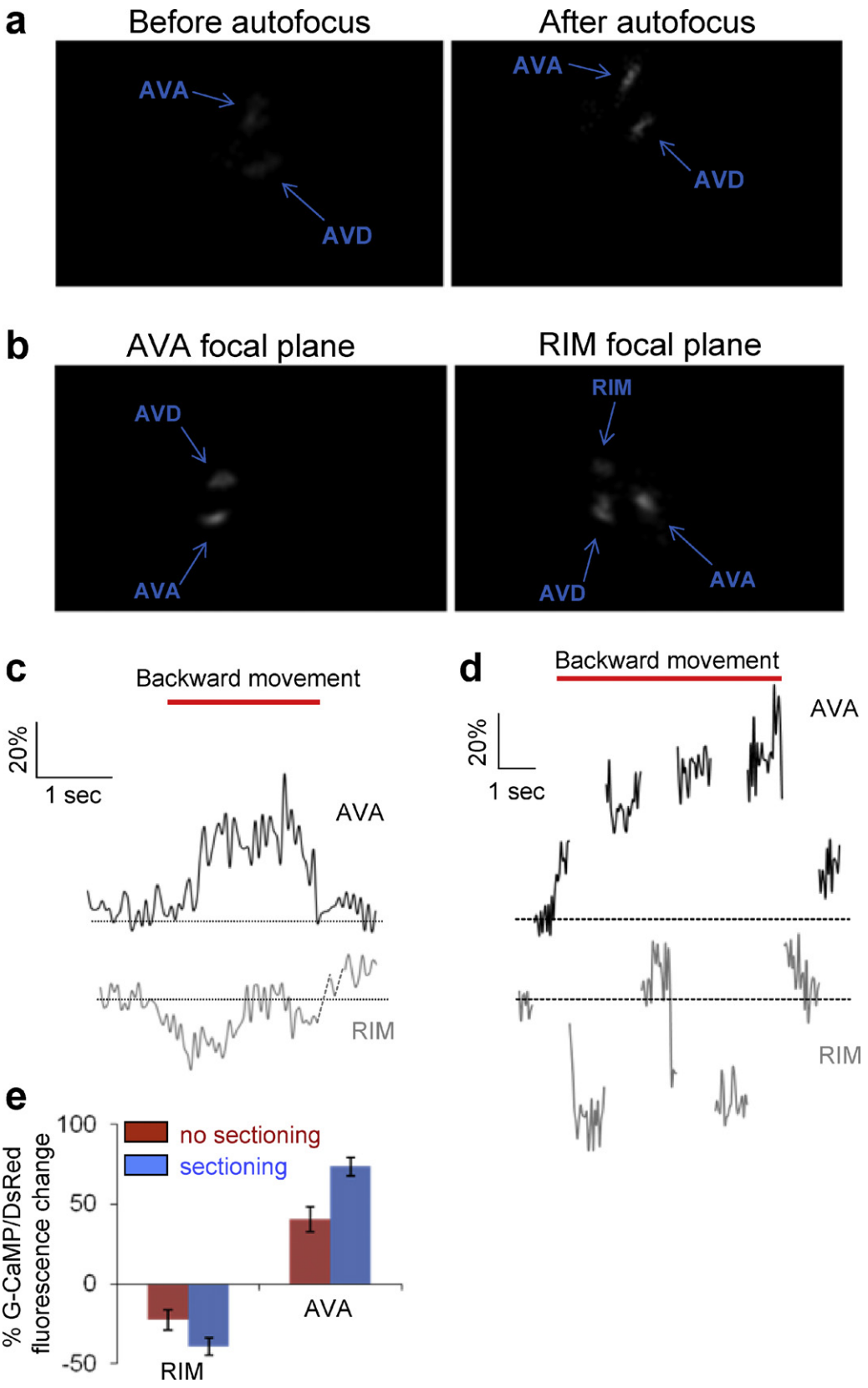


**Fig. 2.** Simultaneous imaging of AVA and RIM in freely behaving nematodes expressing G-CaMP and DsRed. (a) The autofocus function of CARIBN II automatically re-focus images. A day 1 transgenic worm expressing G-CaMP/DsRed2 under the *nmr-1* promoter was tracked for AVA by CARIBN II. The focal plane was manually disturbed (left), which was automatically detected and corrected (right). (b) CARIBN II transversely sections between the AVA (left panel) and RIM (right panel) focal planes. RIM was dim to be visible in the AVA focal plane. (c–e) Calcium activity of AVA and RIM is associated with the same reversal events. (c) AVA and RIM were imaged without enabling the *z*-sectioning function. The red bar denotes backward movement. The dotted lines represent the missing data due to bad quality of images. AVA activity increased while RIM activity decreased in the same reversal. (d) AVA and RIM were imaged through *z*-sectioning. (e) Bar graph of peak/trough percentage of ratio change of G-CaMP/DsRed fluorescence. $n \geq 7$. Error bars: SEM. (For interpretation of the references to color in this figure legend, the reader is referred to the web version of the article.)

surprising that AVA signals were enhanced under the sectioning mode (Fig. 2d and e). Perhaps, in order to get some RIM fluorescence in the same image, AVA was slightly defocused under the non-sectioning mode. We also found that RIM signals fluctuated in long reversals (Fig. 2d), but this was not observed in short reversals shown previously (Piggott et al., 2011). Nevertheless, the above data offer direct evidence that AVA and RIM show activity in the same reversal events, further suggesting that AVA and RIM both contribute to the initiation of reversals. One potential drawback of the *z*-sectioning function is that as the system sectioned along *z*-axis, at any given time point only AVA or RIM was in perfect focus. This left behind some "gaps" in the traces (Fig. 2d). As these "gaps" may occur at different time points in different traces, this shortfall can be partly overcome by examining multiple traces to ensure that one does not miss any event in the "gaps". This new feature nonetheless greatly enhanced the performance of the imaging system.

### 3.3. Conclusion

CARIBN II offers two new features, autofocus and *z*-sectioning, which are not provided by the existing calcium imaging systems developed for freely behaving worms. These features not only greatly improved the overall performance of the imaging system by providing more convenient and smoother data collection and higher signal-to-noise, but also allowed imaging of multiple neurons in the same behavioral task. As this system analyzes worms on the surface of an agar plate in an open environment, sensory stimuli such as mechanical forces and chemicals can be applied to challenge the animals. Thus, this system can also be employed to study how sensory cues modulate circuit activity. CARIBN II will greatly facilitate the dissection of neural circuits controlling behavior in *C. elegans*.

## Acknowledgments

We thank Beverly Piggott for comments and generating the transgenic line; and Loren Looger for G-CaMP3 plasmid. This work was supported grants from Mt. Sinai Foundation (ZF), Pew Scholar Program (XZSX) and the NIGMS (GM083241 to XZSX and ZF).

## Appendix A. Supplementary data

Supplementary data associated with this article can be found, in the online version, at doi:10.1016/j.jneumeth.2012.01.002.

## References

Alkema MJ, Hunter-Ensor M, Ringstad N, Horvitz HR. Tyramine functions independently of octopamine in the *Caenorhabditis elegans* nervous system. Neuron 2005;46:247–60.

Barr MM. Super models. Physiol Genomics 2003;13:15–24.

Ben Arous J, Tanizawa Y, Rabinowitch I, Chatenay D, Schafer WR. Automated imaging of neuronal activity in freely behaving *Caenorhabditis elegans*. J Neurosci Methods 2010;187:229–34.

Cao P, Yuan Y, Pehek EA, Moise AR, Huang Y, Palczewski K, et al. Alpha-synuclein disrupted dopamine homeostasis leads to dopaminergic neuron degeneration in *Caenorhabditis elegans*. PLoS One 2010;5:e9312.

Chalasani SH, Chronis N, Tsunozaki M, Gray JM, Ramot D, Goodman MB, et al. Dissecting a circuit for olfactory behaviour in *Caenorhabditis elegans*. Nature 2007;450:63–70.

Chalfie M, Sulston JE, White JG, Southgate E, Thomson JN, Brenner S. The neural circuit for touch sensitivity in *Caenorhabditis elegans*. J Neurosci 1985;5:956–64.

Faumont S, Rondeau G, Thiele TR, Lawton KJ, McCormick KE, Sottile M, et al. An image-free opto-mechanical system for creating virtual environments and imaging neuronal activity in freely moving *Caenorhabditis elegans*. PLoS One 2011;6:e24666.

Feng Z, Li W, Ward A, Piggott BJ, Larkspur E, Sternberg PW, et al. elegans model of nicotine-dependent behavior: regulation by TRP family channels. Cell 2006;127:621–33.

Gray JM, Hill JJ, Bargmann CI. A circuit for navigation in *Caenorhabditis elegans*. Proc Natl Acad Sci USA 2005;102:3184–91.

Kawano T, Po MD, Gao S, Leung G, Ryu WS, Zhen M. An imbalancing act: gap junctions reduce the backward motor circuit activity to bias *C. elegans* for forward locomotion. Neuron 2011;72:572–86.

Kerr R, Lev-Ram V, Baird G, Vincent P, Tsien RY, Schafer WR. Optical imaging of calcium transients in neurons and pharyngeal muscle of *C. elegans*. Neuron 2000;26:583–94.

Liu J, Ward A, Gao J, Dong Y, Nishio N, Inada H, et al. *C. elegans* phototransduction requires a G protein-dependent cGMP pathway and a taste receptor homolog. Nat Neurosci 2010;13:715–22.

Mori I, Okumura M, Kuhara A. Molecular neurogenetics of sensory behaviors in the hematode *C. elgans*. Nihon Shinkei Seishin Yakurigaku Zasshi 2004;24:239–41.

Piggott BJ, Liu J, Feng Z, Wescott SA, Xu XZS. The neural circuits and synaptic mechanisms underlying motor initiation in *C. elegans*. Cell 2011;147:922–33.

Ward A, Liu J, Feng Z, Xu XZ. Light-sensitive neurons and channels mediate phototaxis in *C. elegans*. Nat Neurosci 2008;11:916–22.

White JG, Southgate E, Thomson JN, Brenner S. The structure of the nervous system of the nematode *Caenorhabditis elegans*. Philos Trans R Soc Lond B 1986;314:1–340.

Whittaker AJ, Sternberg PW. Sensory processing by neural circuits in *Caenorhabditis elegans*. Curr Opin Neurobiol 2004;14:450–6.

Zhang S, Jin W, Huang Y, Su W, Yang J, Feng Z. Profiling a *Caenorhabditis elegans* behavioral parametric dataset with a supervised *K*-means clustering algorithm identifies genetic networks regulating locomotion. J Neurosci Methods 2011;197:315–23.

Zheng Y, Brockie PJ, Mellem JE, Madsen DM, Maricq AV. Neuronal control of locomotion in *C. elegans* is modified by a dominant mutation in the GLR-1 ionotropic glutamate receptor. Neuron 1999;24:347–61.